PHYSICAL REVIEW D **82,** 072005 (2010)

Observation of $B^+ \to \bar{D}^{*0}\tau^+\nu_\tau$ and evidence for $B^+ \to \bar{D}^0\tau^+\nu_\tau$ at Belle

A. Bozek,[30] M. Rozanska,[30] I. Adachi,[8] H. Aihara,[45] K. Arinstein,[1,33] V. Aulchenko,[1,33] T. Aushev,[20,13] T. Aziz,[40] A. M. Bakich,[39] V. Bhardwaj,[35] M. Bischofberger,[26] A. Bondar,[1,33] M. Bračko,[22,14] T. E. Browder,[7] Y. Chao,[29] A. Chen,[27] B. G. Cheon,[6] I.-S. Cho,[49] K.-S. Choi,[49] Y. Choi,[38] J. Dalseno,[23,41] Z. Doležal,[2] Z. Drásal,[2] A. Drutskoy,[4] W. Dungel,[10] S. Eidelman,[1,33] P. Goldenzweig,[4] B. Golob,[21,14] H. Ha,[18] K. Hara,[25] Y. Hasegawa,[37] H. Hayashii,[26] T. Higuchi,[8] Y. Horii,[44] Y. Hoshi,[43] W.-S. Hou,[29] H. J. Hyun,[19] T. Iijima,[25] K. Inami,[25] M. Iwabuchi,[49] Y. Iwasaki,[8] N. J. Joshi,[40] J. H. Kang,[49] P. Kapusta,[30] H. Kawai,[3] T. Kawasaki,[32] H. Kichimi,[8] C. Kiesling,[23] H. O. Kim,[19] J. H. Kim,[17] M. J. Kim,[19] S. K. Kim,[36] Y. J. Kim,[5] B. R. Ko,[18] S. Korpar,[22,14] P. Križan,[21,14] P. Krokovny,[8] T. Kuhr,[16] T. Kumita,[46] A. Kuzmin,[1,33] Y.-J. Kwon,[49] S.-H. Kyeong,[49] M. J. Lee,[36] S.-H. Lee,[18] J. Li,[7] D. Liventsev,[13] R. Louvot,[20] A. Matyja,[30] S. McOnie,[39] H. Miyata,[32] Y. Miyazaki,[25] R. Mizuk,[13] G. B. Mohanty,[40] E. Nakano,[34] M. Nakao,[8] H. Nakazawa,[27] S. Neubauer,[16] S. Nishida,[8] O. Nitoh,[47] T. Nozaki,[8] S. Ogawa,[42] T. Ohshima,[25] S. Okuno,[15] S. L. Olsen,[36,7] W. Ostrowicz,[30] P. Pakhlov,[13] G. Pakhlova,[13] C. W. Park,[38] H. K. Park,[19] R. Pestotnik,[14] M. Petrič,[14] L. E. Piilonen,[48] H. Sahoo,[7] Y. Sakai,[8] O. Schneider,[20] J. Schümann,[8] C. Schwanda,[10] A. J. Schwartz,[4] K. Senyo,[25] J.-G. Shiu,[29] B. Shwartz,[1,33] R. Sinha,[12] P. Smerkol,[14] A. Sokolov,[11] E. Solovieva,[13] M. Starič,[14] J. Stypula,[30] T. Sumiyoshi,[46] G. N. Taylor,[24] Y. Teramoto,[34] I. Tikhomirov,[13] K. Trabelsi,[8] S. Uehara,[8] Y. Unno,[6] S. Uno,[8] G. Varner,[7] K. E. Varvell,[39] K. Vervink,[20] C. H. Wang,[28] M.-Z. Wang,[29] P. Wang,[9] Y. Watanabe,[15] R. Wedd,[24] E. Won,[18] B. D. Yabsley,[39] Y. Yamashita,[31] V. Zhulanov,[1,33] T. Zivko,[14] and A. Zupanc[16]

(Belle Collaboration)

[1]*Budker Institute of Nuclear Physics, Novosibirsk*
[2]*Faculty of Mathematics and Physics, Charles University, Prague*
[3]*Chiba University, Chiba*
[4]*University of Cincinnati, Cincinnati, Ohio 45221*
[5]*The Graduate University for Advanced Studies, Hayama*
[6]*Hanyang University, Seoul*
[7]*University of Hawaii, Honolulu, Hawaii 96822*
[8]*High Energy Accelerator Research Organization (KEK), Tsukuba*
[9]*Institute of High Energy Physics, Chinese Academy of Sciences, Beijing*
[10]*Institute of High Energy Physics, Vienna*
[11]*Institute of High Energy Physics, Protvino*
[12]*Institute of Mathematical Sciences, Chennai*
[13]*Institute for Theoretical and Experimental Physics, Moscow*
[14]*J. Stefan Institute, Ljubljana*
[15]*Kanagawa University, Yokohama*
[16]*Institut für Experimentelle Kernphysik, Karlsruher Institut für Technologie, Karlsruhe*
[17]*Korea Institute of Science and Technology Information, Daejeon*
[18]*Korea University, Seoul*
[19]*Kyungpook National University, Taegu*
[20]*École Polytechnique Fédérale de Lausanne (EPFL), Lausanne*
[21]*Faculty of Mathematics and Physics, University of Ljubljana, Ljubljana*
[22]*University of Maribor, Maribor*
[23]*Max-Planck-Institut für Physik, München*
[24]*University of Melbourne, School of Physics, Victoria 3010*
[25]*Nagoya University, Nagoya*
[26]*Nara Women's University, Nara*
[27]*National Central University, Chung-li*
[28]*National United University, Miao Li*
[29]*Department of Physics, National Taiwan University, Taipei*
[30]*H. Niewodniczanski Institute of Nuclear Physics, Krakow*
[31]*Nippon Dental University, Niigata*
[32]*Niigata University, Niigata*
[33]*Novosibirsk State University, Novosibirsk*
[34]*Osaka City University, Osaka*
[35]*Panjab University, Chandigarh*
[36]*Seoul National University, Seoul*

[37]*Shinshu University, Nagano*
[38]*Sungkyunkwan University, Suwon*
[39]*School of Physics, University of Sydney, NSW 2006*
[40]*Tata Institute of Fundamental Research, Mumbai*
[41]*Excellence Cluster Universe, Technische Universität München, Garching*
[42]*Toho University, Funabashi*
[43]*Tohoku Gakuin University, Tagajo*
[44]*Tohoku University, Sendai*
[45]*Department of Physics, University of Tokyo, Tokyo*
[46]*Tokyo Metropolitan University, Tokyo*
[47]*Tokyo University of Agriculture and Technology, Tokyo*
[48]*IPNAS, Virginia Polytechnic Institute and State University, Blacksburg, Virginia 24061*
[49]*Yonsei University, Seoul*

(Received 13 May 2010; published 11 October 2010)

We present measurements of $B^+ \to \bar{D}^{*0}\tau^+\nu_\tau$ and $B^+ \to \bar{D}^0\tau^+\nu_\tau$ decays in a data sample of 657×10^6 $B\bar{B}$ pairs collected with the Belle detector at the KEKB asymmetric-energy e^+e^- collider. We find 446^{+58}_{-56} $B^+ \to \bar{D}^{*0}\tau^+\nu_\tau$ events with a significance of 8.1 standard deviations, and 146^{+42}_{-41} $B^+ \to \bar{D}^0\tau^+\nu_\tau$ events with a significance of 3.5 standard deviations. The latter signal provides the first evidence for this decay mode. The measured branching fractions are $\mathcal{B}(B^+ \to \bar{D}^{*0}\tau^+\nu_\tau) = (2.12^{+0.28}_{-0.27}(\text{stat}) \pm 0.29(\text{syst}))\%$ and $\mathcal{B}(B^+ \to \bar{D}^0\tau^+\nu_\tau) = (0.77 \pm 0.22(\text{stat}) \pm 0.12(\text{syst}))\%$.

DOI: 10.1103/PhysRevD.82.072005 PACS numbers: 13.20.He, 14.40.Nd

Measurements of leptonic and semileptonic decays of B mesons to the τ lepton can provide important constraints on the standard model (SM) and its extensions. Because of the large mass of the lepton in the final state, these decays are sensitive probes of models with extended Higgs sectors [1]. Semileptonic modes with $b \to c\tau^-\bar{\nu}_\tau$ [2] transitions provide more observables sensitive to new physics than purely leptonic $B^+ \to \tau^+\nu_\tau$ decays. Of particular interest is τ polarization. The effects of new physics are expected to be larger in $B \to \bar{D}\tau^+\nu_\tau$ than in $B \to \bar{D}^*\tau^+\nu_\tau$. We note that decays to the vector meson offer the interesting possibility of studying correlations between the D^* polarization and other observables [3].

The predicted branching fractions, based on the SM, are around 1.4% and 0.7% for $B^0 \to D^{*-}\tau^+\nu_\tau$ and $B^0 \to D^-\tau^+\nu_\tau$, respectively (see, e.g., [4]). Despite relatively large branching fractions, multiple neutrinos in the final states make the search for semitauonic B decays very challenging. Inclusive and semi-inclusive branching fractions have been measured in LEP experiments [5] with an average branching fraction of $\mathcal{B}(b \to \tau\nu_\tau X) = (2.48 \pm 0.26)\%$ [6]. The first exclusive decay was observed by Belle [7] in the $B^0 \to D^{*-}\tau^+\nu_\tau$ mode. Other modes have also been measured by *BABAR* [8] and Belle [9]. The results are still statistically limited. In particular, the Belle preliminary result [9] is the only evidence to date for $B^+ \to \bar{D}^0\tau^+\nu_\tau$. Further improvements in precision could tightly constrain theoretical models.

Decays of B mesons to multineutrino final states can be studied at B factories via the recoil of the accompanying B meson (B_{tag}). Reconstruction of the B_{tag} allows one to calculate the missing four-momentum in the B_{sig} decay; this helps separate signal events from copious backgrounds. At the same time the presence of a B_{tag} strongly suppresses the combinatorial and continuum backgrounds. The disadvantage is the low B_{tag} reconstruction efficiency. To increase statistics, we reconstruct the B_{tag} "inclusively" from all the remaining particles after the B_{sig} selection (see Ref. [7]). A data sample consisting of $657 \times 10^6 B\bar{B}$ pairs is used in this analysis. It was collected with the Belle detector [10] at the KEKB asymmetric-energy e^+e^- (3.5 on 8 GeV) collider [11] operating at the $\Upsilon(4S)$ resonance ($\sqrt{s} = 10.58$ GeV).

We use Monte Carlo (MC) simulations to estimate signal efficiencies and background contributions. Large samples of the signal $B^+ \to \bar{D}^{(*)0}\tau^+\nu_\tau$ decays are generated with the EVTGEN package [12] using the ISGW2 model [13]. Radiative effects are modeled using the PHOTOS code [14]. We use large MC samples of continuum $q\bar{q}$ ($q = u, d, s, c$) and inclusive $B\bar{B}$ events to model the background. The sizes of these samples are, respectively, 6 and 9 times that of the data.

Primary charged tracks are required to have impact parameters consistent with an origin at the interaction point (IP), and to have momenta above 50 MeV/c in the laboratory frame. K^0_S mesons are reconstructed using pairs of charged tracks satisfying $482\ \text{MeV}/c^2 < M_{\pi^+\pi^-} < 514\ \text{MeV}/c^2$ with a vertex displacement from the IP consistent with the reconstructed momentum vector. Muons, electrons, charged pions, kaons, and protons are identified using information from particle identification subsystems [15]. The momenta of particles identified as electrons are corrected for bremsstrahlung by adding photons within a 50 mrad cone along the lepton trajectory.

The π^0 candidates are reconstructed from photon pairs having $118\ \text{MeV}/c^2 < M_{\gamma\gamma} < 150\ \text{MeV}/c^2$. For candidates that share a common γ, we select the one with the

smallest χ^2 value resulting from a π^0 mass-constrained fit. To reduce the combinatorial background, we require that the photons from the π^0 have energies greater than 60–120 MeV, depending on the photon's polar angle. Photons that are not associated with a π^0 are accepted if their energies exceed a polar-angle dependent threshold ranging from 100 to 200 MeV.

The $\bar{D}^0$ candidates are reconstructed in the $K^+\pi^-$ and $K^+\pi^-\pi^0$ final states. We accept $\bar{D}^0$ candidates having an invariant mass in a 3σ window of the nominal M_{D^0} mass.

The $\bar{D}^{*0}$ candidates are reconstructed from $\bar{D}^0\pi^0$. We require that the mass difference $\Delta M = M_{D^*} - M_{D^0}$ be in a 3σ window around its nominal value. We also accept $\bar{D}^0\gamma$ pairs that do not fulfill the requirement on ΔM if they are kinematically consistent with the hypothesis that $\bar{D}^0$ and γ come from the decay $\bar{D}^{*0} \to \bar{D}^0\pi^0$ with one undetected photon ($\gamma_{\rm miss}$) from the π^0 decay ("partial reconstruction" of $\bar{D}^{*0}$). For this purpose $\cos(\theta_{\gamma,\gamma_{\rm miss}})$, the cosine of the angle between two photons from the π^0 is calculated in the $\bar{D}^{*0}$ rest frame taking the nominal $\bar{D}^{*0}$ and π^0 masses. We require $|\cos(\theta_{\gamma,\gamma_{\rm miss}})| < 1.1$ (taking into account experimental precision) and that the energy of the detected photon exceeds 120 MeV. The partial reconstruction of $\bar{D}^{*0}$ increases the reconstruction efficiency by a factor of about 4, but due to higher background it is only used in the subchannels with $\bar{D}^0 \to K^+\pi^-$ decay.

To reconstruct τ lepton candidates, we use the $\tau^+ \to e^+\nu_e\bar{\nu}_\tau$, $\tau^+ \to \mu^+\nu_\mu\bar{\nu}_\tau$, and $\tau^+ \to \pi^+\bar{\nu}_\tau$ modes. In the latter case, we also take into account the contribution from the $\tau^+ \to \rho^+\bar{\nu}_\tau$ channel. The $\tau^+ \to \pi^+\bar{\nu}_\tau$ mode has a sensitivity similar to the $\tau^+ \to e^+\nu_e\bar{\nu}_\tau$ or $\tau^+ \to \mu^+\nu_\mu\bar{\nu}_\tau$ mode, and can be used to study τ polarization. For this channel, due to the higher combinatorial background, we analyze only the decay chains with the $\bar{D}^0 \to K^+\pi^-$ mode. In total, we consider 13 different decay chains, eight with $\bar{D}^{*0}$ and five with $\bar{D}^0$ in the final states.

The signal candidates are selected by combining a $\bar{D}^{(*)0}$ meson with an appropriately charged electron, muon, or pion. In the subchannels with the $\tau^+ \to \pi^+\bar{\nu}_\tau$ decay, the large combinatorial background is suppressed by requiring the pion energy $E_\pi > 0.6$ GeV. From multiple candidates we select a $(\bar{D}^{(*)0}d_\tau^+)$ pair (throughout the paper d_τ stands for the charged τ daughter: e, μ or π) with the best $\bar{D}^{(*)0}$ candidate, based on the value of ΔM (for subchannels where ΔM is available) or M_{D^0}. For pairs sharing the same $\bar{D}^{(*)0}$ candidate, we select the candidate with the largest vertex probability fit on the tagging side.

Once a $B_{\rm sig}$ candidate is found, the remaining particles that are not assigned to $B_{\rm sig}$ are used to reconstruct the $B_{\rm tag}$ decay. The consistency of a $B_{\rm tag}$ candidate with a B-meson decay is checked using the beam-energy constrained mass and the energy difference variables: $M_{\rm tag} = \sqrt{E_{\rm beam}^2 - \mathbf{p}_{\rm tag}^2}$, $\mathbf{p}_{\rm tag} = \sum_i \mathbf{p}_i$, and $\Delta E_{\rm tag} = E_{\rm tag} - E_{\rm beam}$, $E_{\rm tag} = \sum_i E_i$, where $E_{\rm beam}$ is the beam energy and $\mathbf{p}_i$ and E_i denote the 3-momentum vector and energy of the ith particle. All quantities are evaluated in the $\Upsilon(4S)$ rest frame. The summation is over all particles that are assigned to $B_{\rm tag}$. We require that the candidate events have $M_{\rm tag} > 5.2$ GeV$/c^2$ and -0.3 GeV $< \Delta E_{\rm tag} < 0.05$ GeV. With this requirement the $M_{\rm tag}$ distribution of the signal peaks at the B^+ mass with about 80% of the events being contained in the signal-enhanced region $M_{\rm tag} > 5.26$ GeV$/c^2$.

To suppress background and improve the quality of the $B_{\rm tag}$ selection, we impose the following requirements: zero total event charge; no charged leptons in the event (except those coming from the signal side); zero net proton/antiproton number; residual energy in the electromagnetic calorimeter (i.e., the sum of energies that are not included in the $B_{\rm sig}$ nor $B_{\rm tag}$) should be less than 0.35 GeV (0.30 or 0.25 GeV in subchannels with higher backgrounds); the number of neutral particles on the tagging side $N_{\pi^0} + N_\gamma < 6$, $N_\gamma < 3$, and less than four tracks that do not satisfy the requirements imposed on the impact parameters. For decay modes with higher background, we impose further constraints on the total event strangeness and require no K_L^0 in the event. These criteria, which we refer to as "the $B_{\rm tag}$ selection," reject events in which some particles were undetected and suppress events with a large number of spurious showers. In the samples of the $(\bar{D}^{(*)0}l^+)$ pairs ($l = e$, μ), the dominant background comes from semileptonic B decays, $B^+ \to \bar{D}^{(*)0}Xl^+\nu_l$, whereas in the case of $(\bar{D}^{(*)0}\pi^+)$ pairs, the combinatorial background from hadronic B decays dominates.

Further background suppression exploits observables that characterize the signal decay: missing energy $E_{\rm miss} = E_{\rm beam} - E_{\bar{D}^{(*)0}} - E_{d_\tau^+}$; visible energy $E_{\rm vis}$, i.e., the sum of the energies of all particles in the event; the square of missing mass $M_{\rm miss}^2 = E_{\rm miss}^2 - (\mathbf{p}_{\rm sig} - \mathbf{p}_{\bar{D}^{(*)0}} - \mathbf{p}_{d_\tau^+})^2$ and the effective mass of the $(\tau^+\nu_\tau)$ pair, $q^2 = (E_{\rm beam} - E_{\bar{D}^{(*)0}})^2 - (\mathbf{p}_{\rm sig} - \mathbf{p}_{\bar{D}^{(*)0}})^2$ where $\mathbf{p}_{\rm sig} = -\mathbf{p}_{\rm tag}$ [all kinematical variables are in the $\Upsilon(4S)$ rest frame]. The most useful variable for separating signal and background is obtained by combining $E_{\rm miss}$ and $(\bar{D}^{(*)0}d_\tau^+)$ pair momentum: $X_{\rm miss} = (E_{\rm miss} - |\mathbf{p}_{\bar{D}^{(*)0}} + \mathbf{p}_{d_\tau^+}|)/\sqrt{E_{\rm beam}^2 - m_{B^+}^2}$ where m_{B^+} is the B^+ mass. The $X_{\rm miss}$ variable is closely related to the missing mass in the $B_{\rm sig}$ decay but does not depend on the $B_{\rm tag}$ reconstruction [7].

The signal selection criteria are optimized individually in each decay chain, by maximizing the figure of merit, $N_S/\sqrt{N_S + N_B}$, where N_S and N_B are the number of signal and background events in the signal-enhanced region, assuming the SM prediction [4] for the signal branching fractions. The expected background N_B is evaluated using generic MC samples. We require $E_{\rm vis} < 8.3$–8.5 GeV, $E_{\rm miss} > 1.5$–1.9 GeV, and $X_{\rm miss} > 2.0$–2.75 for leptonic τ decays, or $X_{\rm miss} > 1.0$–1.5 for the modes with $\tau \to \pi\nu_\tau$.

In the latter case, where the τ decays to a final state with a single neutrino, we further require $\cos(\theta_{\nu_1\nu_2})$ to be in the range $[-1, 1]$, where $\theta_{\nu_1\nu_2}$ denotes the angle between the two neutrinos in the $(\tau^+\nu_\tau)$ rest frame and is calculated from the $M^2_{\rm miss}$ and q^2 variables. In the sample with $(\bar{D}^0 d^+_\tau)$ pairs, to suppress the cross feeds from the $B \to \bar{D}^* \tau^+ \nu_\tau$ modes, we impose a loose requirement on $q^2 < 9.5\ {\rm GeV}^2/c^4$.

The above requirements result in flat $M_{\rm tag}$ distributions for most background components, while the distribution of the signal modes remains unchanged. The main sources of the peaking background are the semileptonic decays $B^+ \to \bar{D}^{*0} l^+ \nu_l$ and $B \to \bar{D}^{(*)} \pi l^+ \nu_l$ (including $\bar{D}^{**} l^+ \nu_l$).

In order to estimate the peaking background reliably, in particular, from poorly known semileptonic modes of the type $B \to \bar{D}^{**} l \nu_l$, we divide the MC sample into the following categories: $B \to \bar{D}^* l^+ \nu_l$, $B \to \bar{D} l^+ \nu_l$, $B \to \bar{D}^{**} l^+ \nu_l$, other B decays, $c\bar{c}$ and $(u\bar{u} + d\bar{d} + s\bar{s})$ continuum. The normalizations of these components are determined from simultaneous fits to experimental distributions of $M_{\rm tag}$, $\Delta E_{\rm tag}$, E_{d_τ}, $X_{\rm miss}$, $E_{\rm vis}$, q^2, and R_2, the ratio of the second and zeroth Fox-Wolfram moments [16]. These fits are performed separately for the subsamples defined by the $(\bar{D}^{(*)0} d^+_\tau)$ pairs, excluding the region $M_{\rm tag} > 5.26\ {\rm GeV/c^2}$ and $X_{\rm miss} > 2.0$, where we expect enhanced signal contributions. The residual background from $B^0 \to \bar{D}^{*+} \tau^- \nu_\tau$ decays is included in the peaking background component with the decay rate fixed to the PDG value [6].

The signal and combinatorial background yields are extracted from an extended unbinned maximum likelihood fit to the $M_{\rm tag}$ and P_{D^0} [momentum of D^0 from $B_{\rm sig}$ measured in the $\Upsilon(4S)$ frame] variables. The $M_{\rm tag}$ variable allows us to separate the combinatorial background from the signal, while P_{D^0} helps to distinguish between the two signal modes. Correlations between these variables are found to be small.

Parametrizations of two-dimensional probability density functions (PDFs) are determined from the MC samples. They are expressed as the product of one-dimensional PDFs for each variable. The PDFs for $M_{\rm tag}$ of the signal and peaking background components are described using an empirical parametrization introduced by the Crystal Ball Collaboration [17], while combinatorial backgrounds are parametrized by the ARGUS function [18]. It has been empirically found that the PDFs for P_{D^0} are well modeled as a sum of two Gaussian distributions.

The fits are performed in the range $M_{\rm tag} > 5.2\ {\rm GeV}/c^2$, simultaneously to all data subsets. In each of the subchannels, we describe the data as the sum of four components: signal, cross feed between $\bar{D}^{*0}\tau^+\nu_\tau$ and $\bar{D}^0\tau^+\nu_\tau$, combinatorial and peaking backgrounds. The common signal branching fractions $\mathcal{B}(B^+ \to \bar{D}^{*0}\tau^+\nu_\tau)$ and $\mathcal{B}(B^+ \to \bar{D}^0\tau^+\nu_\tau)$, and the numbers of combinatorial background in each subchannel are free parameters of the fit, while the normalizations of peaking background contributions are fixed to the values obtained from the rescaled MC samples (as described above). The signal yields and branching fractions for $B^+ \to \bar{D}^{(*)0}\tau^+\nu_\tau$ decays are related using the following formula, which assumes equal fractions of charged and neutral B meson pairs produced in $\Upsilon(4S)$ decays: $\mathcal{B}(B^+ \to \bar{D}^{(*)0}\tau^+\nu_\tau) = N_s^{D^{(*)}}/(N_{B\bar{B}} \times \sum_k \epsilon_k \mathcal{B}_k)$, where $N_{B\bar{B}}$ is the number of $B\bar{B}$ pairs and the index k runs over the 13 decay chains; ϵ_k denotes the reconstruction efficiency of the specific subchannel and $\mathcal{B}_k$ is the product of intermediate branching fractions. All the intermediate branching fractions are taken from the PDG compilation [6]. The efficiencies of the signal reconstruction, as well as the expected combinatorial and peaking backgrounds, are given in Table I.

The signal extraction procedure has been tested by fitting ensembles of simulated experiments containing all signal and background components. These pseudoexperiments are generated using the shapes of the fitted PDFs for the signal and background components and with the numbers of events that are Poisson distributed around the expected yields. The pull distributions of the extracted signal branching fractions are consistent with standard normal distributions. The small biases in the mean values are included in the final systematic uncertainties. The procedure established above is applied to the data. The $M_{\rm tag}$ and P_{D^0} distributions for the $\bar{D}^{*0}\tau^+\nu_\tau$ and $\bar{D}^0\tau^+\nu_\tau$ samples in data are shown in Fig. 1. The overlaid histograms represent the expected background, scaled to the data luminosity. A clear excess of events over background is visible in the signal-enhanced region.

The branching fractions extracted from the fit are $\mathcal{B}(B^+ \to \bar{D}^{*0}\tau^+\nu_\tau) = (2.12^{+0.28}_{-0.27}({\rm stat}))\%$ and $\mathcal{B}(B^+ \to \bar{D}^0\tau^+\nu_\tau) = (0.77 \pm 0.22({\rm stat}))\%$. The signal yields are

TABLE I. The yields of signal (N_s) and combinatorial background (N_b) events determined from fits to data, number of expected combinatorial ($N_b^{\rm MC}$) and peaking (N_p) background events, signal selection efficiencies ($\epsilon = \sum_k \epsilon_k \mathcal{B}_k$), extracted branching fractions ($\mathcal{B}$) and statistical significances (Σ). N_p and $N_b^{\rm MC}$ are evaluated from fits of the generic MC samples to experimental distributions. The numbers in parentheses refer to the signal $\bar{D}^{*0}(\bar{D}^0)$ modes reconstructed as $\bar{D}^0(\bar{D}^{*0})$. The efficiencies include intermediate branching fractions. The listed errors are statistical only. The results are summed over the considered $\bar{D}^{(*)0}$ and τ decay modes.

Mode	N_s	N_b	$N_b^{\rm MC}$	N_p	$\epsilon(10^{-6})$	$\mathcal{B}(\%)$	$\Sigma(\sigma)$
$\bar{D}^{*0}\tau^+\nu_\tau$	$446^{+58}_{-56}(226)$	1075^{+37}_{-35}	1029 ± 20	31.0 ± 17.7	$32.6 \pm 0.2(16.3)$	$2.12^{+0.28}_{-0.27}$	8.8
$\bar{D}^0\tau^+\nu_\tau$	$146^{+42}_{-41}(15)$	1245^{+40}_{-39}	1310 ± 19	78.2 ± 12.6	$30.0 \pm 0.4(3.2)$	0.77 ± 0.22	3.6

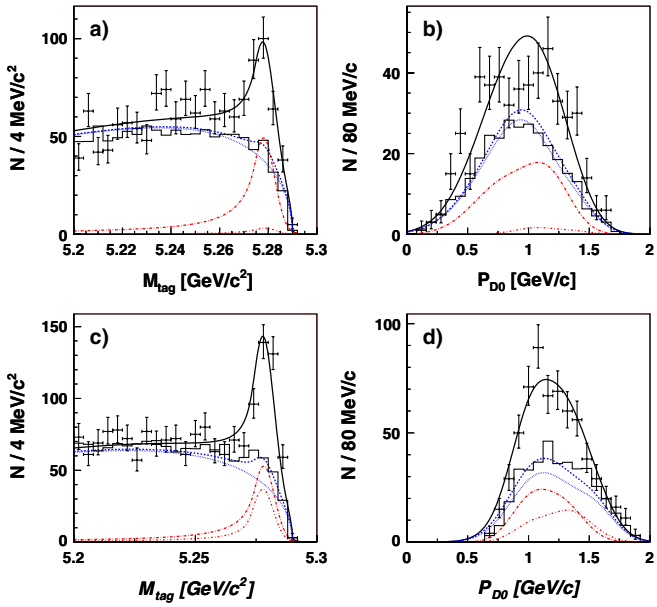

FIG. 1 (color online). The fit projections to $M_{\rm tag}$, and P_{D^0} for $M_{\rm tag} > 5.26$ GeV/c^2 (a),(b) for $\bar{D}^{*0}\tau^+\nu_\tau$, (c),(d) for $\bar{D}^0\tau^+\nu_\tau$. The black curves show the result of the fits. The solid dashed curves represent the background and the dashed dotted ones show the combinatorial component. The dot-long-dashed and dot-short-dashed curves represent, respectively, the signal contributions from $B^+ \to \bar{D}^{*0}\tau^+\nu_\tau$ and $B^+ \to \bar{D}^0\tau^+\nu_\tau$. The histograms represent the MC-predicted background.

446^{+58}_{-56} $B^+ \to \bar{D}^{*0}\tau^+\nu_\tau$ events and 146^{+42}_{-41} $B^+ \to \bar{D}^0\tau^+\nu_\tau$ events. The statistical significances, defined as $\Sigma = \sqrt{-2\ln(\mathcal{L}_0/\mathcal{L}_{\rm max})}$, correspond to 8.8 and 3.6 standard deviations (σ), respectively. Here $\mathcal{L}_{\rm max}$ denotes the maximum likelihood value and $\mathcal{L}_0$ is the likelihood for the zero signal hypothesis, when other signal components are allowed to float. The fitted yields of combinatorial background in the individual submodes are consistent within statistical uncertainties with the MC-based expectations. The fit results are summarized in Table I. The fit projections in $M_{\rm tag}$ and P_{D^0} are shown in Fig. 1.

As a cross-check, we extract the signal yields from an extended unbinned maximum likelihood fit to one-dimensional distributions in $M_{\rm tag}$ and obtain consistent results with the two-dimensional fit. We also examine the distributions of variables used in the signal selection, applying all requirements except those that are related to the considered variable. In all cases the distributions are well reproduced by the sum of signal and background components with normalizations fixed from the fit to the ($M_{\rm tag}$, P_{D^0}) distribution.

The systematic uncertainties in the branching fractions are summarized in Table II. They include uncertainties in the total number of $B\bar{B}$ pairs, the effective efficiencies $\sum_k \epsilon_k \mathcal{B}_k$, and the signal-yield extractions. The systematic uncertainties associated with the effective efficiencies include errors in determination of the efficiencies for $B_{\rm tag}$ reconstruction and $(\bar{D}^{(*)0}d^+_\tau)$ pair selection, coming from efficiencies of tracking, neutral particle reconstruction, particle identification, and from imperfect modeling of real processes. The uncertainty in the $B_{\rm tag}$ and part of the $B_{\rm sig}$ reconstruction efficiency is evaluated from data control samples with $B^+ \to \bar{D}^{*0}\pi^+$ and $B^+ \to \bar{D}^0\pi^+$ decays on the signal side. The absolute normalizations of the data and MC control samples agree to within 13%. The difference, as well as uncertainties in the relative amounts of $D^{*0} - D^0$ cross feeds $\leq 1\%$ are included in the systematic uncertainty of $B_{\rm tag}$ and $B_{\rm sig}$ reconstruction. The latter are evaluated from the sidebands of the ΔE distributions in the $B^+ \to \bar{D}^{*(0)}\pi^+$ control samples. The remaining uncertainties in the lepton identification and signal selection are estimated separately. The latter are determined by comparing MC and data distributions in the variables used for signal selection. The uncertainties due to the partial branching fractions $\mathcal{B}_k$ are taken from the errors quoted by the PDG [6].

TABLE II. Summary of the systematic uncertainties.

Source	$\bar{D}^{*0}\tau^+\nu_\tau$	$\bar{D}^0\tau^+\nu_\tau$
$N_{B\bar{B}}$	$\pm 1.4\%$	$\pm 1.4\%$
Reconstruction of $B_{\rm tag}$ and $B_{\rm sig}$	$\pm 12.9\%$	$\pm 12.8\%$
Lepton id and signal selection	$^{+1.5}_{-1.6}\%$	$^{+4.4}_{-4.5}\%$
Shape of the signal PDFs	$\pm 2.5\%$	$\pm 6.0\%$
Comb. and peaking backgrounds	$\pm 3.3\%$	$\pm 2.7\%$
Fitting procedure	$\pm 0.8\%$	$\pm 1.5\%$
Total	$\pm 13.9\%$	$\pm 15.2\%$

The systematic uncertainties in the signal yield originate from the background evaluation and from the PDF parametrizations of the signal and background components. The resulting error is evaluated from changes in the signal yields obtained from fits where the PDF parameters and the relative contributions of the background components are varied by $\pm 1\sigma$.

All of the above sources of systematic uncertainties are combined together taking into account correlations between different decay chains. The combined systematic uncertainty is 13.9% for the $B^+ \to \bar{D}^{*0}\tau^+\nu_\tau$ mode and 15.2% for $B^+ \to \bar{D}^0\tau^+\nu_\tau$.

We include the effect of systematic uncertainties in the signal yields on the significances of the observed signals by convolving the likelihood function from the fit with a Gaussian systematic error distribution. The significances of the observed signals after including systematic uncertainties are 8.1σ and 3.5σ for the $B^+ \to \bar{D}^{*0}\tau^+\nu_\tau$ and $B^+ \to \bar{D}^0\tau^+\nu_\tau$ modes, respectively.

In conclusion, in a sample of 657×10^6 $B\bar{B}$ pairs we measure branching fractions $\mathcal{B}(B^+ \to \bar{D}^{*0}\tau^+\nu_\tau) = (2.12^{+0.28}_{-0.27}(\text{stat}) \pm 0.29(\text{syst}))\%$, and $\mathcal{B}(B^+ \to \bar{D}^0\tau^+\nu_\tau) = (0.77 \pm 0.22(\text{stat}) \pm 0.12(\text{syst}))\%$, which are consistent within experimental uncertainties with SM expectations [4]. The result on $B^+ \to \bar{D}^0\tau^+\nu_\tau$ is the first evidence for

this decay mode. The branching fraction is consistent with measurements of the related B^0 mode $B^0 \to \bar{D}^- \tau^+ \nu_\tau$, however our result does not support earlier indications of a decay rate larger than the SM expectation [8].

We thank the KEKB group for excellent operation of the accelerator, the KEK cryogenics group for efficient solenoid operations, and the KEK computer group and the NII for valuable computing and SINET3 network support. We acknowledge support from MEXT, JSPS, and Nagoya's TLPRC (Japan); ARC and DIISR (Australia); NSFC (China); MSMT (Czechia); DST (India); MEST, NRF, NSDC of KISTI, and WCU (Korea); MNiSW (Poland); MES and RFAAE (Russia); ARRS (Slovenia); SNSF (Switzerland); NSC and MOE (Taiwan); and DOE (USA).

[1] A. S. Cornell *et al.*, Phys. Rev. D **81**, 115008 (2010), and references quoted therein.
[2] Throughout this paper, the inclusion of the charge-conjugate decay mode is implied unless otherwise stated.
[3] R. Garisto, Phys. Rev. D **51**, 1107 (1995); M. Tanaka, Z. Phys. C **67**, 321 (1995).
[4] C.-H. Chen and C.-Q. Geng, J. High Energy Phys. 10 (2006) 053.
[5] G. Abbiendi *et al.* (OPAL Collaboration), Phys. Lett. B **520**, 1 (2001); R. Barate *et al.* (ALEPH Collaboration), Eur. Phys. J. C **19**, 213 (1996); P. Abreu *et al.* (DELPHI Collaboration), Phys. Lett. B **496**, 43 (2000); M. Acciarri *et al.* (L3 Collaboration), Z. Phys. C **71**, 379 (1996).
[6] C. Amsler *et al.* (Particle Data Group), Phys. Lett. B **667**, 1 (2008).
[7] A. Matyja *et al.* (Belle Collaboration), Phys. Rev. Lett. **99**, 191807 (2007).
[8] B. Aubert *et al.* (*BABAR* Collaboration), Phys. Rev. Lett. **100**, 021801 (2008); Phys. Rev. D **79**, 092002 (2009).
[9] I. Adachi *et al.* (Belle Collaboration), arXiv:0910.4301.
[10] A. Abashian *et al.* (Belle Collaboration), Nucl. Instrum. Methods Phys. Res., Sect. A **479**, 117 (2002).
[11] S. Kurokawa and E. Kikutani, Nucl. Instrum. Methods Phys. Res., Sect. A **499**, 1 (2003), and other papers included in this volume.
[12] D. J. Lange, Nucl. Instrum. Methods Phys. Res., Sect. A **462**, 152 (2001).
[13] D. Scora and N. Isgur, Phys. Rev. D **52**, 2783 (1995).
[14] E. Barberio and Z. Wąs, Comput. Phys. Commun. **79**, 291 (1994).
[15] E. Nakano *et al.*, Nucl. Instrum. Methods Phys. Res., Sect. A **494**, 402 (2002).
[16] G. C. Fox and S. Wolfram, Phys. Rev. Lett. **41**, 1581 (1978).
[17] T. Skwarnicki, Ph.D. thesis, IFJ, Krakow, 1986; DESY Internal Report No. DESY F31-86-02, 1986.
[18] H. Albrecht *et al.* (ARGUS Collaboration), Phys. Lett. B **241**, 278 (1990).